Journal of Bioscience and Bioengineering
VOL. 128 No. 4, 495–503, 2019

ELSEVIER

www.elsevier.com/locate/jbiosc

Osteogenic induction of human mesenchymal stem cells in multilayered electrospun scaffolds at different flow rates and configurations in a perfusion bioreactor

Maliheh Yaghoobi,[1,2] Sameereh Hashemi-Najafabadi,[2,*] Masoud Soleimani,[3] and Ebrahim Vasheghani-Farahani[2]

Engineering Department, Faculty of Chemical Engineering, University of Zanjan, P.O. Box 45371-38791, Zanjan, Iran,[1] Biomedical Engineering Department, Faculty of Chemical Engineering, Tarbiat Modares University, P.O. Box 14115-114, Tehran, Iran,[2] and Hematology Department, Faculty of Medical Sciences, Tarbiat Modares University, P.O. Box 14115- 331, Tehran, Iran[3]

Received 14 November 2018; accepted 20 March 2019
Available online 10 May 2019

Electrospun scaffolds are potentially interesting in bone tissue engineering due to a strong structural similarity to the natural bone matrix. To investigate the osteogenic behavior of cells on the scaffolds, dynamic culture of cells is essential to simulate the biological environment. In the present study, human mesenchymal stem cells (hMSCs) were cultured on multilayer nanohydroxyapatite-polycaprolactone electrospun scaffolds at different configurations (horizontal with or without pressure and parallel with the medium flow) and flow rates in a perfusion bioreactor. Alkaline phosphatase (ALP) activity, cell viability, Ca deposition and RUNX2 expression were determined in three different dynamic states, and compared with static culture after 1, 3, 7, and 14 days. Among dynamic groups, RUNX2 gene expression upregulated more in a horizontal state at a low flow rate without mechanical pressure (LF) and parallel flow (PF), than static group on day 7. At a high flow rate with mechanical pressure, Ca deposition and ALP activity increased 2.34 and 1.7 folds more than in static culture over 7 days, respectively. Furthermore, ALP activity, Ca deposition and RUNX2 gene expression increased in PF samples. PF provided longer culture time with higher cell differentiation. Therefore, high flow rate with mechanical pressure and PF are suggested for producing differentiated cell structure for bone tissue engineering.

[**Key words:** Multilayered electrospun scaffolds; Nanohydroxyapatite-polycaprolactone; Osteogenic differentiation; Perfusion bioreactor; Parallel flow]

Autologous and allogeneic transplantations are commonly used for bone defect repair and regeneration. However, these methods have some limitations such as shortage of donor organs, infection and pain (1,2). To overcome these drawbacks, alternative therapeutic strategies have been developed for bone regeneration. Nowadays, bone grafts with osteoconductive and osteoinductive abilities are rapidly expanding in bone tissue engineering fields.

Electrospun scaffolds are of particular interest for several tissue engineering applications due to cost-effectiveness and convenient fabrication and scale up. They have high specific surface area and good mechanical properties to produce non-woven fibers (3,4). Moreover, electrospun scaffolds can mimic the functionality and morphology of natural bone extracellular matrix (ECM) (5). For instance, to fabricate electrospun scaffolds, the incorporation of nanohydroxyapatite (nHA) into the polycaprolactone (PCL) is promising in bone tissue engineering due to osteoinductivity of nHA and osteoconductivity of PCL. This compound has been extensively studied for bone tissue engineering applications (6–8). Yet, small thickness is one of the obstacles in electrospun scaffolds to be used in deep bone defects. To overcome this limitation, multilayered electrospun constructs can be used for bone tissue engineering. Nonetheless, cell seeding and cell viability within the layered scaffolds are highly challenging in deep structures.

The cells are fed through diffusion transport in static culture, though the diffusion transport is obviously inadequate to keep the cell viability in deep structures (9). Culturing 3-D cellular multilayered scaffolds in perfusion bioreactors is a promising solution to the problem of diffusion in feeding through the constructs (10,11). Furthermore, the mechanical forces play an important role in bone development as hard tissue. Due to the blood and interstitial fluid within the body, shear stresses can stimulate some master osteogenic transcription factors, and contribute to the promotion and mineralization of the bone ECM (12,13).

In our previous work, human mesenchymal stem cells (hMSCs) were cultured on nHA-PCL multilayered electrospun scaffolds at high flow rates in a perfusion bioreactor. Within 3 and 7 days of culture, the results of dynamic state were compared with static culture. hMSCs culture on nHA-PCL multilayered electrospun scaffolds, promoted alkaline phosphatase (ALP) activity of hMSCs and biomineralization of the construct in the perfusion bioreactor (14).

Here, osteogenic differentiation of hMSCs on the multilayered electrospun scaffolds was investigated at both low and high flow rates with three different configurations in a perfusion bioreactor.

* Corresponding author. Tel.: +98 2182884384; fax: +98 2182884931.
E-mail address: s.hashemi@modares.ac.ir (S. Hashemi-Najafabadi).

1389-1723/$ – see front matter
https://doi.org/10.1016/j.jbiosc.2019.03.015

hMSCs were seeded on nHA-PCL electrospun scaffolds and the osteogenic differentiation of cells in three different dynamic cultures were compared with the static one.

MATERIALS AND METHODS

Preparation of electrospun scaffolds The electrospun nHA-PCL scaffolds were produced using PCL (80 kD) (Merck, Darmstadt, Germany) and nHA (< 200 nm) (Sigma–Aldrich, St. Louis, MO, USA) according to the method described in our previous work (14). Briefly, 0.082 g nHA was dispersed in 10 mL chloroform/99.5% *N*,*N*-dimethylformamide (DMF) (Merck) (85/15 v/v), and sonicated for 15 min at 22°C. Chloroform/DMF/nHA dispersion was added to 1.5 g PCL and blended in a magnetic stirrer for 2 h. The suspension was sonicated for 15 min to disperse the nanoparticles in the polymer solution. PCL/nHA scaffolds were fabricated by an electrospinning machine (Nano Azma, Tehran, Iran).

Cell seeding on nHA-PCL scaffolds Primary mesenchymal stem cells, isolated from human adipose tissue, were obtained from Stem Cell Technology Research Center (Tehran, Iran), and were cultured in incomplete medium containing Dulbecco's modified Eagle's medium (DMEM)-Glutamax (Thermo Fisher Scientific, Waltham, MA, USA), 10% fetal bovine serum (FBS) (Bio-Sciences, Dublin, Ireland), 100 U/mL penicillin (Bio-Sciences) and 100 mg/mL streptomycin (Bio-Sciences). The osteogenic medium comprising 0.1 μM dexamethasone (Merck), 10 mM β-glycerophosphate (Merck), and 50 μM ascorbic acid 2-phosphate (Merck), was used as a differentiation medium (complete medium). The fabricated nHA/PCL scaffolds (100–120 μm thick) were cut into circular shapes (8 or 10 mm in diameter for different experiments) and sterilized by immersion in 70% filtered ethanol overnight prior to cell seeding. The constructs were then rinsed twice by phosphate buffer saline (PBS) for 2 h, and were soaked in incomplete medium for 15 min in 48-well plates. Human adipose stem cells (hASCs) (15,000 cells/scaffold) were seeded on the sterilized scaffolds and incubated for 1 h at 37°C and 5% CO_2. Thereafter, incomplete medium up to 500 μL was slowly added to each well while the seeded scaffolds were incubated at 37°C and 5% CO_2 over 2 days to allow for cell attachment.

The design of perfusion bioreactor system The constructed perfusion bioreactor system consisted of four parallel flow chambers (Fig. 1). The bioreactor system included up to four sections: the flow chambers, medium reservoirs (separately for each bioreactor), peristaltic pump and tubes. Each bioreactor comprised the following components: two cylindrical glass chambers (the lower and upper ones), a Teflon screw for connecting the glass chambers, 316 stainless steel support meshes, two silicon O-rings at both sides of the scaffolds to ensure that the only flow path is through the scaffolds without any leakage from the connected chambers, and a cylindrical Teflon piece to hold the scaffolds. Individually, in each flow chamber, the medium was drawn by a multi-channel peristaltic pump from the reservoir, and returned to the same reservoir by silicon tubing (gas permeable to oxygen and carbon dioxide).

Cultivation of multilayer cell-seeded scaffolds with three different configurations The cellular scaffolds (5 layers) with three configurations were placed in the lower chamber, separately. In the first configuration, the scaffolds were compressed under the mechanical pressure between two stainless steel support meshes while the upper chamber was twisted on the lower one by a spiral-shaped Teflon piece to seal the flow chambers (Fig. 1A). Diameter of the scaffolds in the first configuration was 10 mm. In the second configuration, one of the stainless steel support meshes was positioned on the cylindrical Teflon piece (as a holder), and one of the silicon O-rings was placed on the mesh. The cellular scaffolds with 8 mm in diameter were located in the provided space and another stainless steel mesh support and silicon O-ring were stacked, respectively. Ultimately, flow chambers were assembled and sealed using a spiral-shaped Teflon piece (Fig. 1B). The third configuration was different from the others in which the scaffolds were placed vertically inside the lower chamber. In this configuration, the hollow cylindrical Teflon piece was inserted in the lower chamber on which one of the silicon O-rings was placed. The stainless steel support mesh was then positioned on the silicon O-rings and the cellular scaffolds were located vertically in the chamber. Thereafter, the silicon O-rings were placed on the support and the upper chamber twisted on the lower chamber by Teflon spiral-shaped piece (Fig. 1C). Diameter of the scaffolds in the third configuration was the same as the first configuration. The bioreactor system inside the incubator is shown in Fig. 1D.

In the first configuration, the cellular scaffolds were under compression between two stainless steel mesh supports when the chambers were sealed using a Teflon screw. In the second configuration, the cellular scaffolds were not under compression due to the fact that they were placed in the space created by the stainless steel mesh support and O-ring. In addition, the layers were placed on top of each other and did not have full freedom to move. The depth of the free space was about 0.5 mm for movement of the cellular scaffolds. It was only possible to have a very small collision between the upper layer and stainless steel mesh support, and a very small collision between lower and upper cellular layers under the culture medium flow. In the third configuration, the cellular scaffolds were stacked together outside of the bioreactors and transferred inside the hollow cylindrical Teflon piece in the lower chamber of each bioreactor. The hollow cylindrical Teflon piece was similar to a cylinder with perforated floor and cellular scaffolds were placed

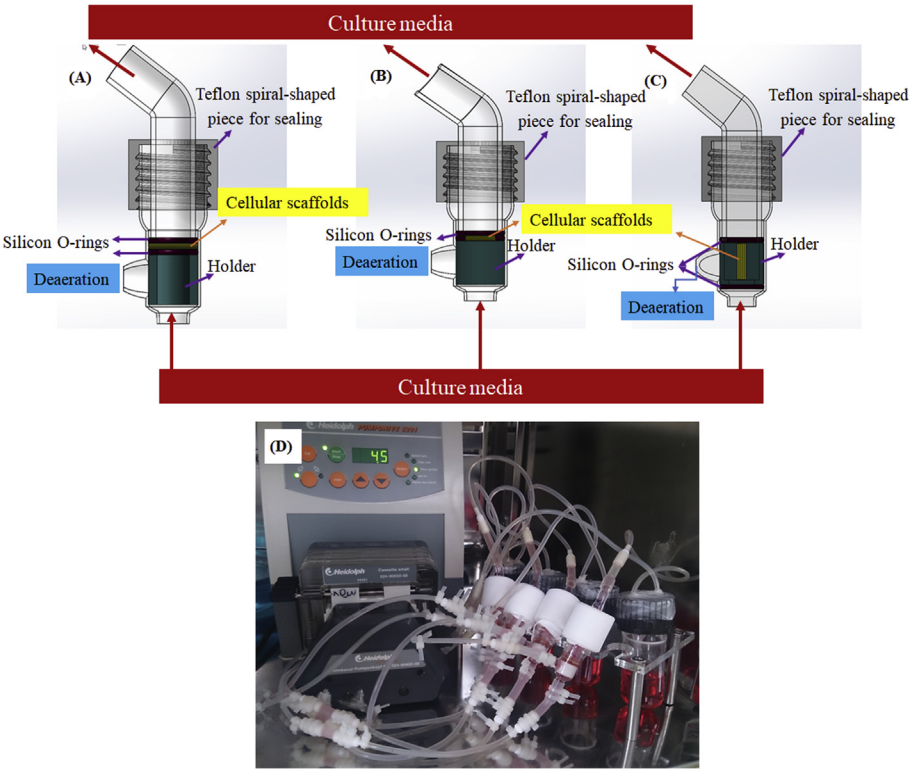

FIG. 1. A schematic picture of three configurations for dynamic cultures. (A) Cellular scaffolds without mechanical pressure. (B) Cellular scaffolds with mechanical pressure. (C) Cellular scaffolds parallel with the medium flow without mechanical pressure. (D) The bioreactor system in the incubator.

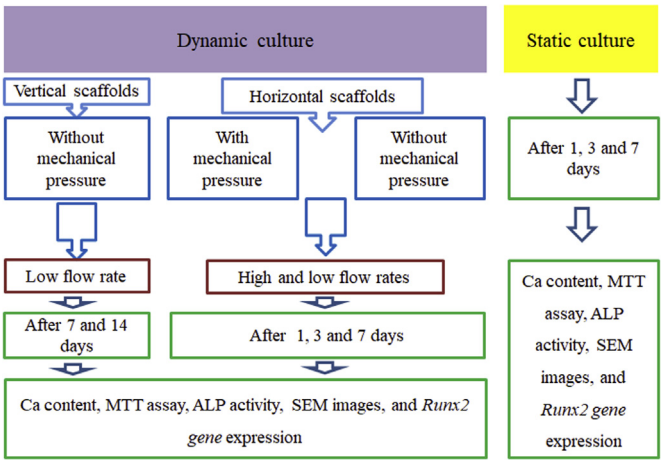

FIG. 2. Flow diagram of the experiments (high and low flow rates).

vertically in a hole in bottom of the hollow cylindrical Teflon piece. The culture medium flow was upward for each bioreactor in all the configurations. In third configuration, the flow rate of the culture medium was not so high that could move the cellular scaffolds. So, at the end of each experiment, the cellular scaffolds were still located vertically on the hole in the bottom of the hollow cylindrical Teflon piece.

To investigate the effect of high and low flow rates, the complete medium was pumped from the reservoirs through the bioreactors employing a multichannel peristaltic pump (Heidolph Instruments, Schwabach, Germany) at two flow rates of 4.5 and 2 mL/min. In the third configuration, the low flow rate (2 mL/min) was applied. The medium was replaced every 2–3 days. The cultivated cellular scaffolds were harvested after 1, 3, and 7 days for cell viability, ALP activity, calcium content assay, scanning electron microscopy (SEM) analysis and real-time reverse transcriptase-polymerase chain reaction (RT-PCR) (for RUNX2 gene expression). For the third configuration, cell viability, ALP activity, SEM analysis and RUNX2 gene expression were evaluated on days 7 and 14. In parallel to all dynamic tests, static condition was also examined. The flow diagram of the experiments is illustrated in Fig. 2.

The average pore size and porosity was measured and reported in our previous work (Yaghoobi et al. (14)). The average porosity was 76.6 ± 2.39%, and the average pore size of 60 selected pores from three SEM images was 15.77 ± 1.53 μm.

MTT assay The viability analysis of cultured hASCs on nHA/PCL scaffolds was determined by MTT assay (15) after 1, 3, and 7 days (n = 3). The cellular scaffolds were rinsed with serum-free medium, followed by addition of MTT-DMEM solution (50 μL MTT solution and 500 μL DMEM) to each well of 48-well plates, and then incubated at humidified incubator (37°C and 5% CO_2) for 4 h. After removing the medium, insoluble purple formazan granules were dissolved in dimethyl sulfoxide (500 mL/well) and the absorbance was measured by an automatic microplate reader (ELX 800, Bio-Tek Instruments, Winooski, VT, USA) at 570 nm.

ALP activity The osteogenic ability of hASC cultured under static and dynamic conditions was determined after 1, 3, and 7 days (n = 3) by measuring ALP activity of the cells (16). The cell lysates were extracted by cell lysis buffer containing protease inhibitor followed by rinsing the cellular scaffolds with PBS. Fifty milliliter of cell lysates was mixed with 100 mL *p*-nitrophenyl phosphate (pNPP) (1 mg/mL) in 1 M diethanolamine buffer containing 0.5 mM $MgCl_2$, pH 9.8. The absorbance of the final solution was measured at 405 nm following incubation at 37°C for 30 min. ALP activity was normalized to total protein, which was determined using bicinchoninic acid (BCA) protein assay Kit (Thermo Fisher Scientific).

Calcium deposition assay Calcium content of the cellular constructs was assessed using a colorimetric assay (17,18) by cresolphthalein complexone (CPC) Kit (Pars Azmoon, Tehran, Iran) after 1, 3 and 7 days of culture (n = 3). Briefly, 1 mL of 0.6 N hydrochloric acid (HCL) was added to the constructs after washing with calcium-free PBS to dissolve the calcium deposition. Then, 20 μL of the solution (containing calcium deposition) was added to 1 mL solution containing 0.06 mM 2-CPC, 7 mM 8-hydroxyquinoline, detergents, 0.8 M ethanolamine (pH 10.7), and 20 mM HCL (pH 1.1). The absorbance of the samples was measured at 570 nm following incubation at 37°C for 30 min.

Scanning electron microscopy In order to qualitatively evaluate the calcium deposition on the cellular scaffolds, the scaffolds were inspected after 7 days of culture in different conditions. In brief, the constructs were rinsed twice with calcium-free PBS and fixed with 2.5% glutaraldehyde at 4°C for 1 h. Then, the samples were dehydrated with gradient ethanol (50%, 70%, 80%, 90%, and 100%). The layers of the construct were then separated from each other following drying. Prior to SEM analysis, the dried samples were coated with a thin layer of gold. SEM images were taken using a SEM instrument (LEO 1450VP, Carl Zeiss, Oberkochen, Germany).

TABLE 1. The primer sequences and product size for real-time RT-PCR reactions.

Gene	Primer sequence	Product size (bps)
RUNX2	F: TCTTAGAACAAATTCTGCCCTTT R: TGCTTTGGTCTTGAAATCACA	136
β-Actin	F: TGAAGATCAAGATCATTGCTCCTC R: AGTCATAGTCCGCCTAGAAGC	168

Real-time reverse transcriptase-polymerase chain reaction The expression level of Runt-related transcription factor 2 (RUNX2, osteogenesis-related gene) was measured using RT-PCR. Total RNA was manually extracted from each construct (19) by RNX-Plus solution (Sinaclon, Tehran, Iran), and analyzed according to the manufacturer's protocol. The concentration of extracted RNA quantified by measuring the optical density (OD) at 260 nm using a BioPhotometer Plus (Eppendorf, Hamburg, Germany), and the purity was verified by the OD_{260}/OD_{280} ratio. The extracted RNA was then used for cDNA synthesis (Vivantis, Selangor Darul Ehsan, Malaysia). The quantitative RT-PCR analysis of RUNX-2 genes was performed on StepOnePlus real time PCR system (Applied Biosystems, Foster City, CA, USA) using SYBR Premix Ex Taq II (Takara, Shiga, Japan), under the following cycle parameters: hot start at 95°C for 30 s followed by 40 cycles of 95°C for 5 s, 60°C for 35 s, and 60°C for 60 s. The primers for the target and housekeeping genes are listed in Table 1. Up- or down-regulation of gene expression was analyzed using 2- (-ΔΔCt) method. Finally, the results were corrected by β-actin (exogenous control) expression levels, and normalized with respect to the values on day 0 of culture.

Statistical data analysis Experimental results were analyzed using one-way ANOVA and Tukey's multiple comparisons test in GraphPad Prism 7.03. The significance level was set at minimum p-value < 0.05. The results were expressed as mean ± standard deviation (SD), n = 3.

RESULTS

Cell viability The effect of two different horizontal states on cell viability at high and low flow rates of culture medium in the bioreactors was compared with the static culture after 1, 3, and 7 days. Moreover, the effect of parallel flow on the cell viability at a low flow rate was evaluated in the third configuration, and compared with the static culture after 7 and 14 days. While cell viability decreased after 7 days in HF group, the static group reached the maximum cell viability, higher than the other groups on day 7 (Fig. 3A). As seen in Fig. 3A, the increase of optical density over 7 days of culture was not significant in dynamic states with mechanical pressure at high and low flow rates. Furthermore, the cell viability decreased at low and high flow rate conditions without mechanical pressure from day 1–7 (with p-values of 0.0003 and 0.0114 for HF and LF, respectively). Nevertheless, the proliferation noticeably increased in static state (from day 1–7, p-value < 0.002) with a significant difference between the static and dynamic cultures over time (p-value < 0.05) (Fig. 3A). While the decrease in cell viability of PF group was not significant, cell viability of static samples was significantly increased from day 7–14 (p-value = 0.019) (Fig. 3B). Moreover, a significant difference can be seen between the static and dynamic cultures on day 14 (p-value = 0.0009).

ALP activity ALP activity of the cells in the constructs, as an early marker of osteoblastic differentiation (20), was determined and normalized to total protein content. The relative ALP activity (ALP activity to total protein) is illustrated in Fig. 4A for two horizontal configurations of dynamic and static cultures after 1, 3, and 7 days. ALP activity of all samples increased notably throughout the culture time. A significant difference was observed between days 3 and 7 at the high flow rate with mechanical pressure (HFWP) (p-value = 0.0056) and the significant difference (p-value = 0.0314) for LFWP group was also observed between days 3 and 7. Additionally, no significant difference was found among the other samples on day 7 when

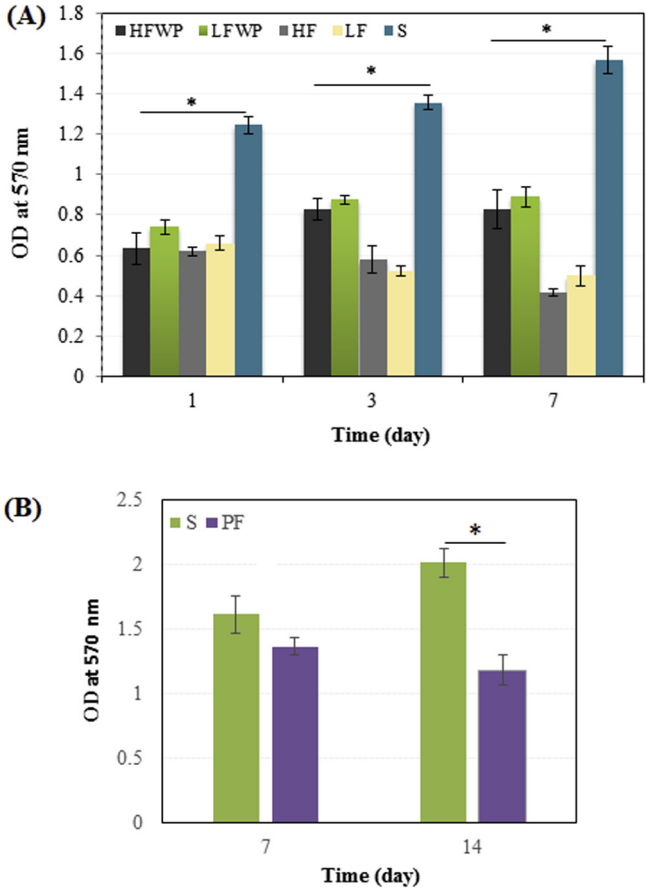

FIG. 3. (A) Viability of MSCs on the multilayer scaffolds in a perfusion bioreactor (dynamic culture) in two horizontal configurations and static culture after 1, 3, and 7 days. All results are shown as average ± standard deviation; n = 3. All dynamic samples differ significantly, when compared to the static sample (*p-value < 0.05). (B) Viability of MSCs on the multilayered scaffolds in a perfusion bioreactor in parallel state after 7 and 14 (*p-value = 0.0009) days of culture. HFWP, high flow rate with mechanical pressure; LFWP, low flow rate with mechanical pressure; HF, high flow rate without mechanical pressure; LF, low flow rate without mechanical pressure; PF, parallel flow; S, static.

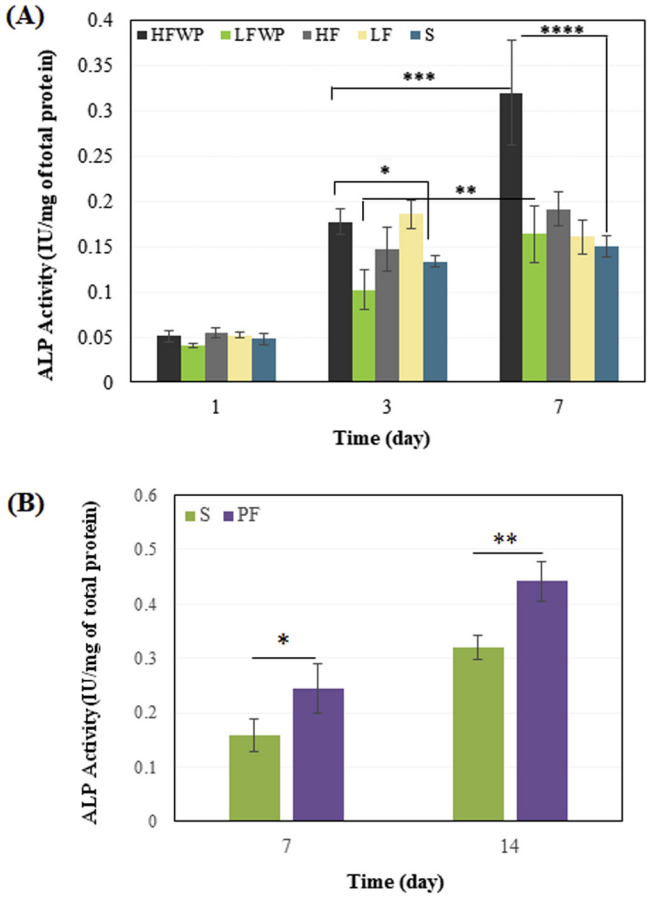

FIG. 4. (A) ALP activity of hMSCs on the multilayered constructs in the perfusion bioreactor with two horizontal configurations compared to the static condition. Difference between HFWP and S was significant on day 3 (*p-value < 0.05). For HFWP and LFWP, differences between days 3 and 7 were significant (**, ***p-value < 0.05). Difference between HFWP and S was significant on day 7 (****p-value < 0.05). (B) ALP activity of MSCs on the multilayered constructs parallel with the medium flow into the bioreactor, in comparison with the static condition after 7 and 14 days show significant differences. *, **p-value < 0.03 between two conditions of static and PF on days 7 and 14, respectively. HFWP, high flow rate with mechanical pressure; LFWP, low flow rate with mechanical pressure; HF, high flow rate without mechanical pressure; LF, low flow rate without mechanical pressure; PF, parallel flow; S, static.

compared to static state, except for HFWP and S (p-value = 0.0005). The mechanical pressure at low flow rate did not show any significant effect on ALP activity. Moreover, ALP activity increased significantly in parallel cellular scaffolds (third configuration), relative to static condition on days 7–14 (Fig. 4B).

Calcium deposition Calcium deposition was determined in the cultured hMSCs on multilayered electrospun scaffolds after 1, 3, and 7 days of culture using a colorimetric assay. Fig. 5A reveals that the calcium content in different dynamic and static conditions distinctly increased over the culture time. Comparing two horizontal dynamic states at low and high flow rates indicated that the calcium deposition on compact scaffolds was higher at the high flow rate when compared to other groups on days 3 and 7 (p-value < 0.0001). Moreover, the mineralized matrix content increased significantly at the high flow rate with mechanical pressure (HFWP) in comparison with other states after 3 and 7 days of culture. Additionally, the calcium deposition on cellular scaffolds in parallel flow increased with respect to the static condition from day 7–14 (Fig. 5B).

SEM analysis SEM was used to evaluate the mineral deposition on cellular multilayered electrospun scaffolds with three different configurations in the bioreactors and static culture after 7 days of culture. The mineralization of some parts of cellular scaffolds is shown in Fig. 6. The SEM results revealed that HFWP group dramatically improved the calcium deposition on the cultured cells on scaffolds in comparison with the static condition. In the configuration with mechanical pressure, the cellular scaffolds had a compact structure, therefore, the separation of attached layers was challenging. In cellular scaffolds, at the high flow rate with mechanical pressure (HFWP), the mineralized matrix extended further than low flow rate with mechanical pressure. This phenomenon was also observed in the configuration without mechanical pressure, though mineralization at HFWP sample was generally higher than other dynamic groups. In PF group, as seen in Fig. 6, some mineralized areas of the cellular scaffolds were denser than those at the static condition, but morphology of the mineralized cellular scaffolds in the PF group did not resemble the other dynamic groups.

Effect of the flow rate on RUNX2 expression Fig. 7 shows the variation of RUNX2 expression as a master gene for osteogenic differentiation in dynamic and static groups after 3 and 7 days of culture (Fig. 7A). In addition, in parallel state, RUNX2 expression was evaluated in comparison with S after 7 and 14 days of culture (Fig. 7B). The expression of RUNX2 was

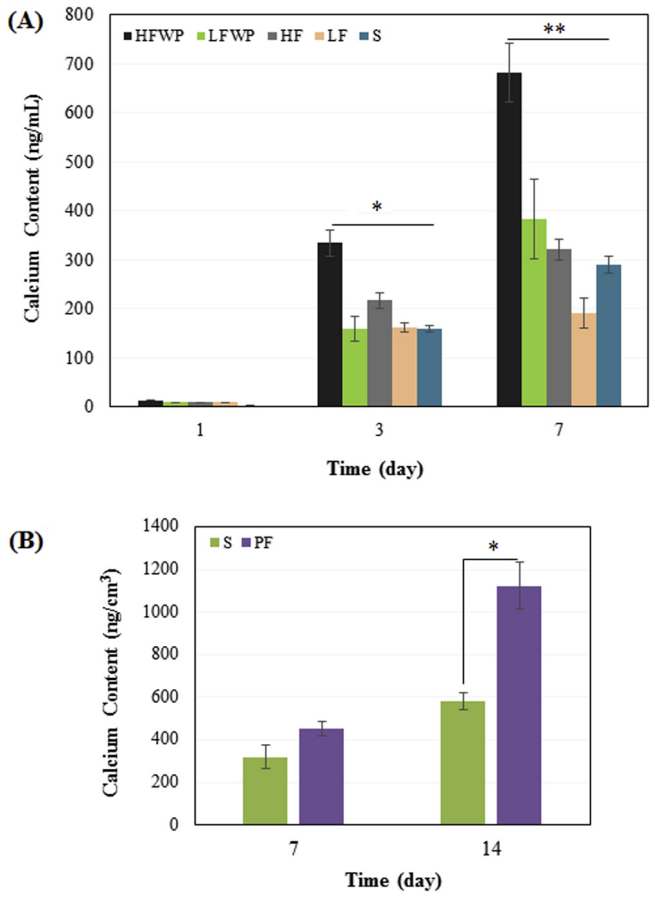

FIG. 5. (A) The quantification of mineralization (Ca content) in constructs at different conditions after 1, 3 and 7 days of culture. *p-value < 0.05 and **p-value < 0.03 indicate significant differences between HFWP and the other groups after 3 and 7 days of culture, respectively. (B) Calcium deposition on parallel cellular scaffolds shows a significant difference (*p-value < 0.02) between two samples after 14 day of culture, compared with the static samples from day 7–14. HFWP, high flow rate with mechanical pressure; LFWP, low flow rate with mechanical pressure; HF, high flow rate without mechanical pressure, LF, low flow rate without mechanical pressure, PF, parallel flow; S, static.

upregulated within all groups where some revealed a significant increase after 7 days of culture except for HFWP group. RUNX2 expression increased in dynamic groups, with a significant difference between the static and LF groups (p-value < 0.0001), and also between LFWP and static groups (p-value $= 0.0041$) on day 7. The relative expression of RUNX2 gene in HF and static groups remained approximately the same after 7 days of culture.

The HF group showed down-regulation of RUNX2 after 3 days of culture. Interestingly, RUNX2 gene showed a high upregulation from day 3–7 in constructs at the low flow rate without mechanical pressure (p-value < 0.05). Moreover, the relative expression of RUNX2 gene in PF was upregulated higher than the static condition after 7 and 14 days of culture. These results suggested that the low flow rate of culture medium played a significant role in improving and accelerating the RUNX2 expression, while it may have an adverse effect at high flow rates in HF group. In addition, the expression of RUNX2 was more upregulated in LF than in PF after 7 days of culture.

DISCUSSION

Electrospun scaffolds with high surface area-to-volume ratio, high porosity, and morphological properties similar to bone ECM, are promising for bone tissue engineering (21–23), yet their low thickness limits their application in deep bone defects. To tackle this problem, multilayered scaffolds with higher thickness can be applied. The static culture condition is not adequate to feed these cellular structures. The perfusion bioreactors have been widely employed to improve nutrient transfer within thick scaffolds in *in vitro* studies (24–26). In addition, the medium flow in the bioreactors has been proved to facilitate and enhance the osteogenic differentiation by applying suitable mechanical stimuli (27).

To the best of our knowledge, there is no published literature on osteogenic behavior of multilayered cellular electrospun scaffolds in perfusion bioreactors. In this study, three different configurations of multilayer scaffolds in the perfusion bioreactor were used to assess the osteogenic differentiation of MSCs on nHA-PCL electrospun scaffolds. In the first configuration, the multilayered cellular scaffolds were placed between two mesh supports with mechanical pressure (compact multilayer). In the second configuration, internal pieces (O-rings, mesh supports, and polytetrafluoroethylene holder) of the glass chamber were assembled to make the cellular scaffolds without mechanical pressure. Finally, in the third configuration, the medium flow was parallel with the scaffolds.

Srouji et al. (28) employed the electrospun PCL-collagen type I scaffolds with 30 layers to estimate the osteogenic differentiation of human MSCs (hMSCs) seeded on the scaffolds in a PluriX plug-flow bioreactor. They made a hole centered on each scaffold (apparently for flowing media), and used culture medium at a flow rate of 6.4 mL min^{-1}. They showed that dynamic culture can promote osteogenic differentiation on cellular electrospun scaffolds. Here, electrospun nHA-PCL scaffolds were used without manipulation of their structure (without the hole), while the flow perfused throughout the scaffolds in a compact multilayered construct.

Due to the low pore size of scaffolds, optimization or setting an appropriate flow rate of culture medium is an important task in multilayered electrospun scaffolds inside the perfusion bioreactor. A high flow rate of the medium may cause washout phenomenon (29). During washout, the cells lose their attachment to the scaffolds and intracellular connections, and furthermore, the osteogenic differentiation decreases (30).

In the present study, two levels of flow rates were evaluated (2 and 4.5 mL min^{-1}). According to the pre-test results (not presented here), the medium flow stopped at flow rates less than 2 mL min^{-1}, while approximately 40–50% of the cells were washed out, at flow rates higher than 4.5 mL min^{-1}. Hence, two levels of flow rates were applied to compare osteogenic ability of MSCs in this condition. In addition, as described above, two configurations were considered to estimate the pressure force effect on early osteoblast differentiation.

In comparison to the static condition, cell viability was not sufficient in dynamic groups. The population of cells decreased dramatically within all dynamic groups on day 1. This result may imply that from the very first of medium pumping, some cells presumably cannot withstand the flow rate and survive on the scaffolds. However, after 1 day, they adapted themselves to the new condition and could proliferate slightly. The second reason for this trend may be clogging of some pores in each layer, overlaid by compression, in the first configuration. Additionally, in the second configuration, the collision between cellular scaffolds and with the upper mesh support was inevitable. High porosity and large pore size provide enough space for cell proliferation. As shown in Fig. 3A, the flow rate had no effect on the cell numbers in the first and second configurations during the culture time. In other words, the increase in the number of cells was not significant between low and high flow rates in the first configuration. Gomes et al. (31) compared fiber mesh scaffolds with different porosity produced from starch and PCL, for proliferation and osteogenic differentiation of bone marrow stromal cells. They showed that cell viability was significantly higher in scaffolds with

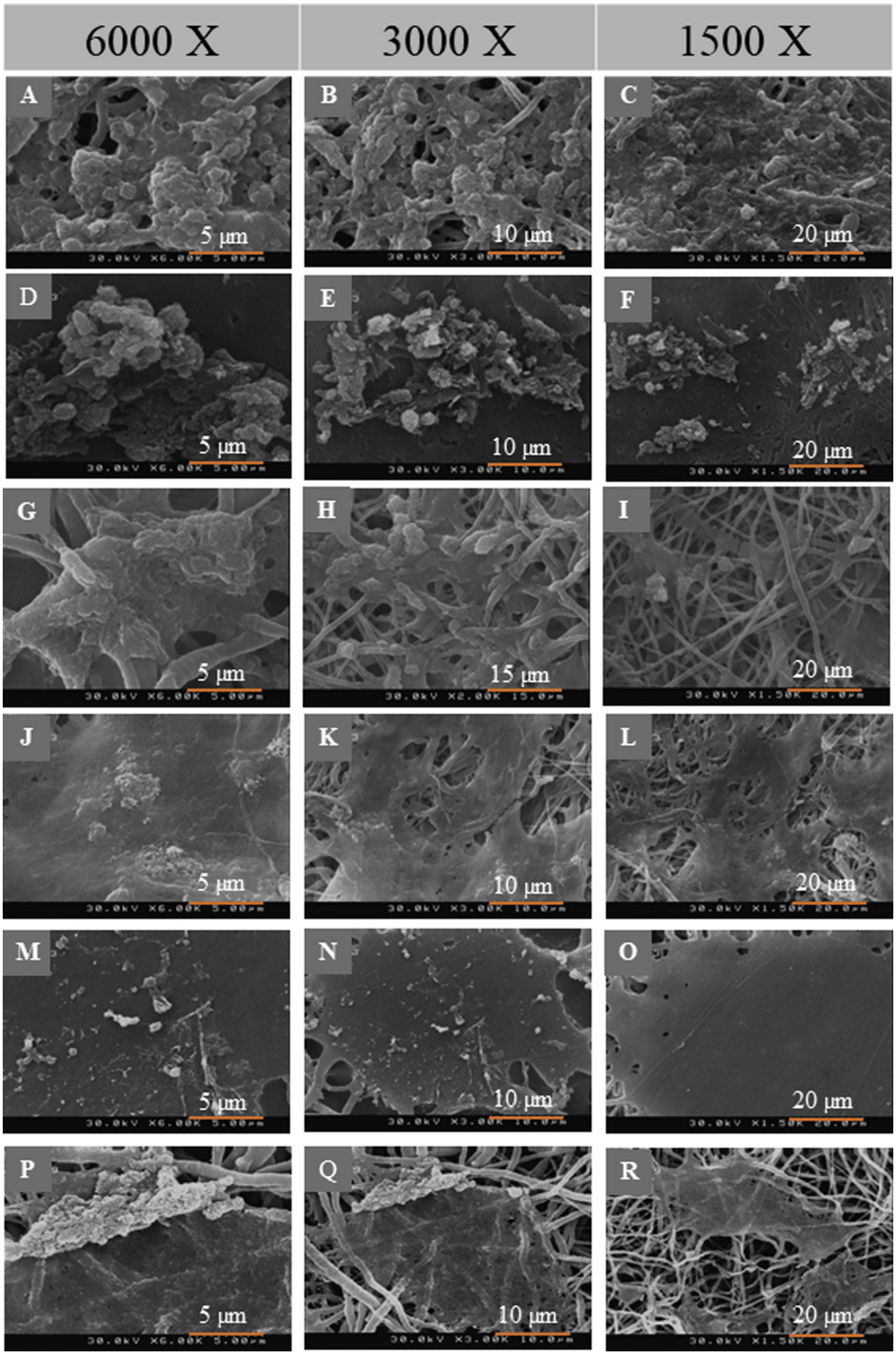

FIG. 6. SEM images of cellular multilayered electrospun scaffolds in dynamic and static cultures after 7 day of culture with three magnifications (left to right: 5, 10, and 20 μm). HFWP (A–C); LFWP (D–F); HF (G–I); LF (J–L); S (M–O); PF (P–R). HFWP, high flow rate with mechanical pressure; LFWP, low flow rate with mechanical pressure; HF, high flow rate without mechanical pressure; LF, low flow rate without mechanical pressure; PF, parallel flow.

75% porosity than that of 50% in both static and dynamic cultures. Therefore, the porosity of construct can affect and decrease cell viability and proliferation due to compactness of the layers. However, compared to the static condition, ALP activity was higher in HFWP group (Fig. 4). As an ectoenzyme, ALP is an important marker of *in vitro* osteogenation (32). Moreover, it plays a significant role in hard tissue formation, since it can increase the local concentration of inorganic phosphate and initiate matrix mineralization (33). To study the development of osteogenic differentiation, mRNA or protein expression of ALP can be estimated, although ALP activity is the most conventional method (34). Our results revealed that dynamic flow rate with or without mechanical pressure, can affect ALP activity (14), which is consistent with previous studies. The reports on the dynamic culture of MSCs indicated that shear stress can promote and

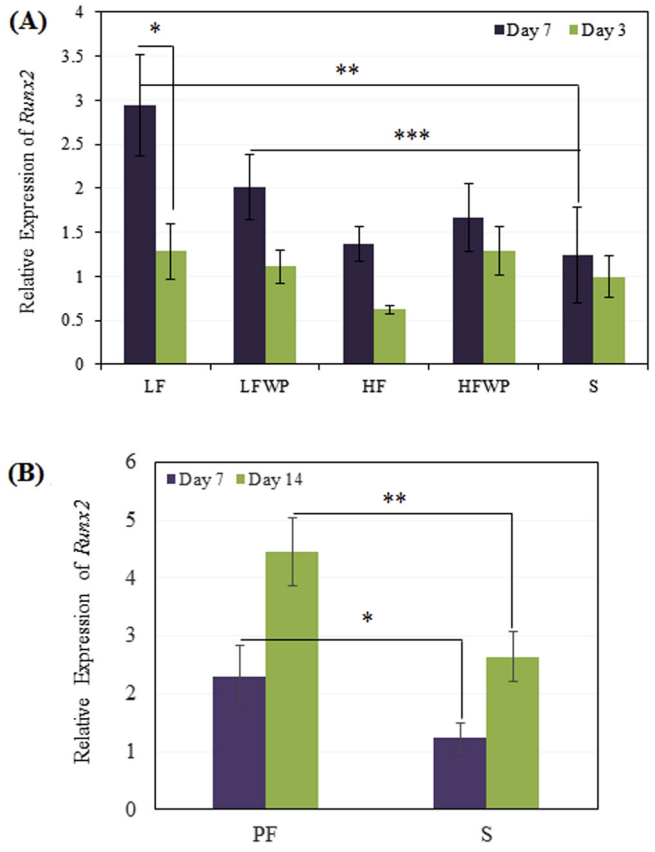

FIG. 7. (A) Relative expression of RUNX2 gene in dynamic and static culture groups after 3 and 7 days of culture. The real-time RT-PCR values were corrected by β-actin expression levels, and normalized with respect to the values on day 0 of culture. The difference in expression of RUNX2 gene for LF between days 3 and 7 was significant (*p-value < 0.03). **, ***p-value < 0.05 indicates significant differences between S and other two groups (LF and LFWP) on day 7. (B) Comparison of parallel cellular scaffolds with static condition after 7 and 14 days of culture. PF and static conditions had significant difference after 7 and 14 days of culture. All values are shown as average ± standard deviation; n = 3 (p-value < 0.05).

facilitate osteogenic differentiation due to the medium perfusion. In addition, the perfusion flow provides sufficient nutrients for the cells in comparison with static culture (35–37).

Here, Ca^{2+} content of each sample was measured using a colorimetric assay to compare the mineral content of each construct in three configurations with the static culture (38). To verify the mineralization, SEM imaging (39,40) was used to observe the mineralized surface of constructs. The results indicated an integrated structure in cellular scaffolds cultured under mechanical pressure with a high flow rate. It seems that the secreted proteins on mineralized ECM could produce adhesive layers similar to a thick cohesive layer with differentiated cells after 7 days. Thus, in bone tissue engineering, the multilayered scaffolds are more preferable than single-layer ones due to their easier use for filling the bone defects as a result of their high thickness and strength. Overall, the mineralization was significantly higher in HFWP group compared with other groups, suggesting that the high dynamic flow rate with compression enhanced the mineralization on the structure (Fig. 5). Mechanical forces play an essential role in remodeling and development of bone due to the promotion of osteogenic master genes and mineral deposition (41). There are some *in vitro* studies that corroborate the effect of fluid flow or mechanical forces on development of osteogenesis. To estimate osteoblastic differentiation, marrow stromal osteoblasts were cultured on titanium fiber mesh scaffolds under perfusion flow at different flow rates. The results showed that the cellular scaffolds at the highest flow rate had more calcium deposition on day 8 than in static culture (42,43). Dahlin et al. (44) studied the mineralized matrix of co-cultures of human umbilical vein endothelial cells (HUVECs) and human MSCs, on PCL electrospun scaffolds under the perfusion flow of culture medium. They showed that co-cultures of hMSCs and HUVECs could not promote the mineralization while the culture of hMSCs alone under the flow perfusion increased calcium deposition (44). Furthermore, as proved in several studies, composite electrospun scaffold of nHA-PCL is a suitable construct for bone regeneration by MSCs (7,45). nHA has several roles in bone implants, among which osteoinductive is of great importance in terms of improving the surface properties. Therefore, it is assumed that by changing the surface charge, nHA can induce the scaffold to adsorb some chemical components and improve the mineralization (46), and consequently affect the surface morphology. The surface morphology may vary depending on different flow patterns (parallel or perpendicular to the surface of the scaffold).

RUNX2 gene expression is another factor to study the osteogenic process due to the fact that the upstream osteoblastic differentiation in osteogenic process is conducted by RUNX2 by inducing the expression of osteoblast specific genes during osteoblast maturation (47). Therefore, RUNX2 plays a critical role in regulation and progression of osteoblast differentiation during osteogenesis (48). Zou et al. (49) generated RUNX2-yellow fluorescent protein (YFP) reporter to compare the osteogenesis ability of human embryonic stem cells (hESCs) with osteoprogenitor cells from bone marrow cells. They demonstrated that RUNX2-YFP reporter system is a satisfactory tool for evaluation of osteogenic differentiation. Moreover, shear stress can affect RUNX2 gene expression due to the fluid flow. Sellgren and Ma (50) seeded 3D chitosan composite scaffolds with hMSCs and placed them under two flow configurations (the cellular construct was perfused either under transverse flow or parallel flow). Their results indicated that shear stress influenced the expression of RUNX2 and other osteoblast genes due to the fluid flow (50). As evident in Fig. 7A, the expression of RUNX2 gene in dynamic samples was greater than that in the static ones on day 7, and the highest expression of RUNX2 gene in dynamic groups is associated with the cellular scaffolds cultured at the low flow rate without mechanical pressure on day 7. These results showed that dynamic flow can increase and improve the expression of RUNX2 gene due to shear stress from the medium flow, while high flow rate may have lower effect. In addition, the medium flow in PF, improved the expression of RUNX2 gene more than that one in S, on days 7 and 14; however, LF group had the highest expression among all groups on day 7. The parallel flow created forces to prevent the cell attachments. This flow pattern affected gene expression and other cell functions in the early days of cultivation and differentiation. Following the cell proliferation and differentiation on the multilayers, in HFWP group, and as a result of clogging the pores in the scaffolds due to mineralization and secretion of the cellular matrix, prolonged cell culture was difficult. However, due to the existing flow pattern in PF, clogging the pores was lower and it showed prolonged cell culture until 14 days. But as the dynamic culture accelerates osteogenic differentiation in each flow pattern, it seems that the maturation time of the cells in the bioreactors will be shorter than normal mode or static condition.

This study investigated the cell viability, calcium deposition (both quantitative and qualitative), ALP activity, and RUNX2 gene expression to evaluate the osteogenic differentiation of MSCs in three different configurations, seeded on multilayered electrospun nHA-PCL scaffolds in a perfusion bioreactor under different flow rates. Except for the cell viability, all aforementioned factors increased in HFWP group in comparison with the static condition. In this group, higher cell differentiation was obtained under the introduced mechanical pressure. The production of a compact

differentiated cell structure in the first configuration with high flow rate in the bioreactor was one of the most significant achievements of this study. Moreover, the medium flow in PF condition, improved the osteogenic cell differentiation more than other dynamic states. Evidently, the production of differentiated cell scaffolds in this configuration takes less time than in static culture. Therefore, PF can be proposed as a potential alternative for bone tissue engineering applications.

ACKNOWLEDGMENTS

We thank Tarbiat Modares University for supporting this work. This research was also supported by Iran National Science Foundation (INSF) under grant No. 92006873, Tehran, Iran. The authors declare that they have no conflicts of interest.

References

1. **Baroli, B.:** From natural bone grafts to tissue engineering therapeutics: brainstorming on pharmaceutical formulative requirements and challenges, J. Pharm. Sci., **98**, 1317–1375 (2009).
2. **Reichert, J. C., Cipitria, A., Epari, D. R., Saifzadeh, S., Krishnakanth, P., Berner, A., Woodruff, M. A., Schell, H., Mehta, M., Schuetz, M. A., Duda, G. N., and Hutmacher, D. W.:** A tissue engineering solution for segmental defect regeneration in load-bearing long bones, Sci. Transl. Med., **4**, 141ra93 (2012).
3. **Di Martino, A., Liverani, L., Rainer, A., Salvatore, G., Trombetta, M., and Denaro, V.:** Electrospun scaffolds for bone tissue engineering, Musculoskelet. Surg., **95**, 69–80 (2011).
4. **Huang, Z. M., Zhang, Y. Z., Kotaki, M., and Ramakrishna, S.:** A review on polymer nanofibers by electrospinning and their applications in nanocomposites, Compos. Sci. Technol., **63**, 2223–2253 (2003).
5. **Sell, S. A., Wolfe, P. S., Garg, K., McCool, J. M., Rodriguez, I. A., and Bowlin, G. L.:** The use of natural polymers in tissue engineering: a focus on electrospun extracellular matrix analogues, Polymers, **2**, 522–553 (2010).
6. **Doustgani, A., Vasheghani-Farahani, E., Soleimani, M., and Hashemi-Najafabadi, S.:** Optimizing the mechanical properties of electrospun polycaprolactone and nanohydroxyapatite composite nanofibers, Compos. Part B Eng., **43**, 1830–1836 (2012).
7. **Qian, J., Xu, M., Suo, A., Yang, T., and Yong, X.:** An innovative method to fabricate honeycomb-like poly(ε-caprolactone)/nano-hydroxyapatite scaffolds, Mater. Lett., **93**, 72–76 (2013).
8. **Sultana, N. and Khan, T. H.:** Polycaprolactone scaffolds and hydroxyapatite/polycaprolactone composite scaffolds for bone tissue engineering, J. Bionanosci., **7**, 169–173 (2013).
9. **Kleinhans, C., Mohan, R. R., Vacun, G., Schwarz, T., Haller, B., Sun, Y., Kahlig, A., Kluger, P., Finne-Wistrand, A., Walles, H., and Hansmann, J.:** A perfusion bioreactor system efficiently generates cell-loaded bone substitute materials for addressing critical size bone defects, Biotechnol. J., **10**, 1727–1738 (2015).
10. **Gaspar, D. A., Gomide, V., and Monteiro, F. J.:** The role of perfusion bioreactors in bone tissue engineering, Biomatter, **2**, 167–175 (2012).
11. **Yeatts, A. B. and Fisher, J. P.:** Bone tissue engineering bioreactors: dynamic culture and the influence of shear stress, Bone, **48**, 171–181 (2011).
12. **Nguyen, B. N., Ko, H., and Fisher, J. P.:** Tunable osteogenic differentiation of hMPCs in tubular perfusion system bioreactor, Biotechnol. Bioeng., **113**, 1805–1813 (2016).
13. **Romagnoli, C. and Brandi, M. L.:** Adipose mesenchymal stem cells in the field of bone tissue engineering, World J. Stem Cells, **6**, 144–152 (2014).
14. **Yaghoobi, M., Hashemi-Najafabadi, S., Soleimani, M., Vasheghani-Farahani, E., and Mousavi, S. M.:** Osteogenic differentiation and mineralization on compact multilayer nHA-PCL electrospun scaffolds in a perfusion bioreactor, Iran. J. Biotechnol., **14**, 41–49 (2016).
15. **Vistica, D. T., Skehan, P., Scudiero, D., Monks, A., Pittman, A., and Boyd, M. R.:** Tetrazolium-based assays for cellular viability: a critical examination of selected parameters affecting formazan production, Cancer Res., **51**, 2515–2520 (1991).
16. **Birmingham, E., Niebur, G. L., McHugh, P. E., Shaw, G., Barry, F. P., and McNamara, L. M.:** Osteogenic differentiation of mesenchymal stem cells is regulated by osteocyte and osteoblast cells in a simplified bone niche, Eur. Cells Mater., **23**, 13–17 (2012).
17. **Leary, N. O., Pembroke, A., and Duggan, P. F.:** Single Stable reagent (Arsenazo III) for optically robust measurement of calcium in serum and plasma, Clin. Chem., **38**, 904–908 (1992).
18. **Munoz-Pinto, D. J., Jimenez-Vergara, A. C., Hou, Y., Hayenga, H. N., Rivas, A., Grunlan, M., and Hahn, M. S.:** Osteogenic potential of poly(ethylene glycol)–poly(dimethylsiloxane) hybrid hydrogels, Tissue Eng. Part A, **18**, 1710–1719 (2012).
19. **Yu, C., Young, S., Russo, V., Amsden, B. G., and Flynn, L. E.:** Techniques for the isolation of high-quality RNA from cells encapsulated in chitosan hydrogels, Tissue Eng. Part C Methods, **19**, 829–838 (2013).
20. **Chen, Y., Huang, Z., Li, X., Li, S., Zhou, Z., Zhang, Y., Feng, Q. L., and Yu, B.:** In vitro biocompatibility and osteoblast differentiation of an injectable chitosan/nano-hydroxyapatite/collagen scaffold, J. Nanomater., **2012**, 401084 (2012).
21. **Jang, J. H., Castano, O., and Kim, H. W.:** Electrospun materials as potential platforms for bone tissue engineering, Adv. Drug Deliv. Rev., **61**, 1065–1083 (2009).
22. **Liao, S., Murugan, R., Chan, C. K., and Ramakrishna, S.:** Processing nano-engineered scaffolds through electrospinning and mineralization suitable for biomimetic bone tissue engineering, J. Mech. Behav. Biomed. Mater., **1**, 252–260 (2008).
23. **Prabhakaran, M. P., Venugopal, J., and Ramakrishna, S.:** Electrospun nanostructured scaffolds for bone tissue engineering, Acta Biomater., **5**, 2884–2893 (2009).
24. **Beşkardeş, I. G., Aydın, G., Bektaş, S., Cengiz, A., and Gümüşderelioğlu, M.:** A systematic study for optimal cell seeding and culture conditions in a perfusion mode bone-tissue bioreactor, Biochem. Eng. J., **132**, 100–111 (2018).
25. **Di Buduo, C. A., Soprano, P. M., Tozzi, L., Marconi, S., Auricchio, F., Kaplan, D. L., and Balduini, A.:** Modular flow chamber for engineering bone marrow architecture and function, Biomaterials, **146**, 60–71 (2017).
26. **Mitra, D., Whitehead, J., Yasui, O. W., and Leach, J. K.:** Bioreactor culture duration of engineered constructs influences bone formation by mesenchymal stem cells, Biomaterials, **146**, 29–39 (2017).
27. **Vetsch, J. R., Müller, R., and Hofmann, S.:** The evolution of simulation techniques for dynamic bone tissue engineering in bioreactors, J. Tissue Eng. Regen. Med., **9**, 903–917 (2013).
28. **Srouji, S., Kizhner, T., Suss-Tobi, E., Livne, E., and Zussman, E.:** 3-D Nanofibrous electrospun multilayered construct is an alternative ECM mimicking scaffold, J. Mater. Sci. Mater. Med., **19**, 1249–1255 (2008).
29. **Holtorf, H. L., Jansen, J. A., and Mikos, A. G.:** Flow perfusion culture induces the osteoblastic differentiation of marrow stromal cell-scaffold constructs in the absence of dexamethasone, J. Biomed. Mater. Res. A, **72**, 326–334 (2005).
30. **Zhang, Z. Y., Teoh, S. H., Teo, E. Y., Khoon Chong, M. S., Shin, C. W., Tien, F. T., Choolani, M. A., and Chan, J. K.:** A comparison of bioreactors for culture of fetal mesenchymal stem cells for bone tissue engineering, Biomaterials, **31**, 8684–8695 (2010).
31. **Gomes, M. E., Holtorf, H. L., Reis, R. L., and Mikos, A. G.:** Influence of the porosity of starch-based fiber mesh scaffolds on the proliferation and osteogenic differentiation of bone marrow stromal cells cultured in a flow perfusion bioreactor, Tissue Eng., **12**, 801–900 (2006).
32. **da Silva, H. M., Mateescu, M., Damia, C., Champion, E., Soares, G., and Anselme, K.:** Importance of dynamic culture for evaluating osteoblast activity on dense silicon-substituted hydroxyapatite, Colloids Surf. B Biointerfaces, **80**, 138–144 (2010).
33. **Golub, E. E. and Boesze-Battaglia, K.:** The role of alkaline phosphatase in mineralization, Curr. Opin. Orthop., **18**, 444–448 (2007).
34. **Granéli, C., Thorfve, A., Ruetschi, U., Brisby, H., Thomsen, P., Lindahl, A., and Karlsson, C.:** Novel markers of osteogenic and adipogenic differentiation of human bone marrow stromal cells identified using a quantitative proteomics approach, Stem Cell Res., **12**, 153–165 (2014).
35. **Kanda, Y., Nishimura, I., Sato, T., Katayama, A., Arano, T., Ikada, Y., and Yoshinari, M.:** Dynamic cultivation with radial flow bioreactor enhances proliferation or differentiation of rat bone marrow cells by fibroblast growth factor or osteogenic differentiation factor, Regen. Ther., **5**, 17–24 (2016).
36. **Nishimura, I., Hisanaga, R., Sato, T., Arano, T., Nomoto, S., Ikada, Y., and Yoshinari, M.:** Effect of osteogenic differentiation medium on proliferation and differentiation of human mesenchymal stem cells in three-dimensional culture with radial flow bioreactor, Regen. Ther., **2**, 24–31 (2015).
37. **van den Dolder, J., Bancroft, G. N., Sikavitsas, V. I., Spauwen, P. H., Jansen, J. A., and Mikos, A. G.:** Flow perfusion culture of marrow stromal osteoblasts in titanium fiber mesh, J. Biomed. Mater. Res. A, **64**, 235–241 (2003).
38. **de Girolam, L., Sartori, M. F., Albisetti, W., and Brini, A. T.:** Osteogenic differentiation of human adipose-derived stem cells: comparison of two different inductive media, J. Tissue Eng. Regen. Med., **1**, 154–157 (2007).
39. **Koroleva, A., Deiwick, A., Nguyen, A., Schlie-Wolter, S., Narayan, R., Timashev, P., Popov, V., Bagratashvili, V., and Chichkov, B.:** Osteogenic differentiation of human mesenchymal stem cells in 3-D Zr-Si organic inorganic scaffolds produced by two-photon polymerization technique, PLoS One, **10**, e0118164 (2015).
40. **Lobo, S. E. and Arinzeh, T. L.:** Biphasic calcium phosphate ceramics for bone regeneration and tissue engineering applications, Materials (Basel), **3**, 815–826 (2010).
41. **Hung, B. P., Hutton, D. L., and Grayson, W. L.:** Mechanical control of tissue-engineered bone, Stem Cell Res. Ther., **4**, 10 (2013).

42. **Bancroft, G. N., Sikavitsas, V. I., van den Dolder, J., Sheffield, T. L., Ambrose, C. G., Jansen, J. A., and Mikos, A. G.:** Fluid flow increases mineralized matrix deposition in 3D perfusion culture of marrow stromal osteoblasts in a dose-dependent manner, Proc. Natl. Acad. Sci. USA, **99**, 12600–12605 (2002).
43. **Sikavitsas, V. I., Bancroft, G. N., Holtorf, H. L., Jansen, J. A., and Mikos, A. G.:** Mineralized matrix deposition by marrow stromal osteoblasts in 3D perfusion culture increases with increasing fluid shear forces, Proc. Natl. Acad. Sci. USA, **100**, 14683–14688 (2003).
44. **Dahlin, R. L., Gershovich, J. G., Kasper, F. K., and Mikos, A. G.:** Flow perfusion co-culture of human mesenchymal stem cells and endothelial cells on biodegradable polymer scaffolds, Ann. Biomed. Eng., **42**, 1381–1390 (2014).
45. **Hassan, M. I., Sultana, N., and Hamdan, S.:** Bioactivity assessment of poly(ε-caprolactone)/hydroxyapatite electrospun fibers for bone tissue engineering application, J. Nanomater., **2014**, 573238 (2014).
46. **Venugopal, J., Prabhakaran, M. P., Zhang, Y., Low, S., Choon, A. T., and Ramakrishna, S.:** Biomimetic hydroxyapatite-containing composite nanofibrous substrates for bone tissue engineering, Philos. Trans. R. Soc. A, **368**, 2065–2081 (2010).
47. **Bruderer, M., Richards, R. G., Alini, M., and Stoddart, M. J.:** Role and regulation of RUNX2 in osteogenesis, Eur. Cells Mater., **28**, 269–286 (2014).
48. **James, A. W.:** Review of signaling pathways governing MSC osteogenic and adipogenic differentiation, Scientifica, **2013**, 684736 (2013).
49. **Zou, L., Kidwai, F. K., Kopher, R. A., Motl, J., Kellum, C. A., Westendorf, J. J., and Kaufman, D. S.:** Use of RUNX2 expression to identify osteogenic progenitor cells derived from human embryonic stem cells, Stem Cell Rep., **4**, 190–198 (2015).
50. **Sellgren, K. L. and Ma, T.:** Effects of flow configuration on bone tissue engineering using human mesenchymal stem cells in 3D chitosan composite scaffolds, J. Biomed. Mater. Res. A, **103**, 2509–2520 (2014).